

Preparation of novel porous solids from alumina-pillared fluorine
micas by acid-treatment

Tomohiro Yamaguchi, Teruyoshi Yoshimura, Tomohiko Yamakami,
Seiichi Taruta, Kunio Kitajima

Department of Chemistry and Material Engineering,
Faculty of Engineering, Shinshu University,
4-17-1, Wakasato, Nagano-shi 380-8553

Corresponding author:

Tomohiro Yamaguchi

mtmouth@shinshu-u.ac.jp

TEL +81-26-269-5417, FAX +81-26-269-5415

Abstract

New porous solids from alumina-pillared fluorine micas (APMs), which were obtained from synthetic Na-tetrasilicic fluorine mica [$\text{NaMg}_{2.5}\text{Si}_4\text{O}_{10}\text{F}_2$], were prepared by sulfuric acid-treatment under mild conditions at 25°C . The products were investigated by XRD, ICP, SEM, TEM and N_2 adsorption-desorption isotherm at 77 K. XRD measurements indicated that the interlayer pillared structure having a large basal spacing collapsed during the early stages of the acid-treatment. ICP analyses indicated that Al^{3+} and Mg^{2+} ions were leached out from the pillared micas during the acid-treatment. The pore properties of the leached products were found to differ from those of the mother pillared micas: the acid leaching of the pillared micas leads to the formation of mesopores around 3.2 nm in diameter. The correlation between the change in pore properties and cation elution behavior suggests that the mesopore formation results from the leaching of Mg^{2+} ions from the octahedral sheet of the pillared micas. The leached products thus obtained retained the flaky morphology of the mother pillared micas. These results show that the mild acid-treatment using APMs provides a novel route for obtaining unique mesopore solids having the large particle sizes of the mother micas.

Keywords: Layered materials, Intercalation, Alumina-pillared fluorine mica, Acid-treatment, Mesopore

1. Introduction

Several methods are known for the fabrication of porous materials from clay minerals. Oxide-pillared clays, a type of microporous ceramic materials, are produced from swellable clay minerals by the intercalation of bulky inorganic polycations into their interlayer regions and subsequent heat treatment. On heating, the polycations in the interlayer regions are converted into thermally stable oxides that prop the layers apart as pillars. Oxide-pillared fluorine micas [1-8] are obtained from swellable fluorine micas [9-12] as host crystals, in the same way as from natural clay minerals. The swellable micas show such features as high crystallinity, large cation exchange capacity and high thermal durability. The pillared micas thus obtained retain features of the host micas and hence have cation exchangeability [4]. Unique mica ceramics with micropores were obtainable by sintering of the pillared fluorine mica powders at low temperatures around 500-700°C [2,5,6].

Selective leaching of clay minerals is another method for preparing porous materials. Acid-treatment of various clay minerals, such as kaolinite [13,14], phlogopite [15,16], vermiculite [17], montmorillonite [18,19], fluorohectorite [15], talc [20,21], chlorite [22], saponite [23,24], has been reported. The acid-treated products typically show micro- or mesopores, depending on the starting clay mineral species and the acid-treatment conditions. Generally, a high acid concentration and/or elevated temperature are employed for the acid-treatment conditions so that the

acid-leached products consist mainly of silica because the other constituents are leached out almost completely.

In contrast to the acid leaching of such clay minerals, when pillared micas are used as starting material, rather mild acid-treatment conditions may be employed to modify the microporous structure. This is because interlayer micropores act as a diffusion path to access the internal surface of the silicate layers and hence the leaching process may occur at the micropore surface, i.e., the internal surface of the silicate flakes. This internal diffusion may allow the pore properties of the pillared micas to be altered under milder acid-treatment conditions than usual. Recently, Ishii et al. [25] reported the preparation of highly porous silica products from vermiculite and tetraethoxysilane or methyltriethoxysilane using a pillaring method combined with acid leaching. However, as far as we know, the report on the acid-treatment of alumina-pillared clays to modify pore properties, especially to form mesopores, has been lacking. Thus, the present work investigates sulfuric acid-treatment of alumina-pillared fluorine micas (APMs) at 25°C under different conditions to modify their porous properties and establish a new route for the preparation of novel porous solids using pillared micas. For reference, the host mica prior to pillaring was also treated with sulfuric acid in the same manner. The acid-treated products were characterized by XRD, ICP, SEM, TEM and nitrogen adsorption-desorption.

2. Experimental

Na-tetrasilicic fluorine mica (Na-TSM) having an anhydrous structural formula of $\text{NaMg}_{2.5}\text{Si}_4\text{O}_{10}\text{F}_2$ was used as host crystal for the preparation of APMs [2-4,6]. Na-TSM was synthesized by a procedure described previously [4]. The polyhydroxoaluminum (PHA) solution used as a pillaring agent was prepared by the Al metal dissolving method [26]. The solution had an OH/Al ratio of 2.50 and an Al concentration of 6.05 mol/L. A suspension containing mica crystals was allowed to react with the diluted PHA solution at 65°C for 24 h under vigorous stirring with a solution loading of 44.8 mmol (Al)/1.0 g-mica. The solution loading employed in the present study was referred to our previous report [4]. The product was washed several times, dried at 65°C and then calcined at 350, 500 or 700°C for 2 h to obtain APMs (hereafter abbreviated, e.g., APM-500 for the pillared mica obtained by calcination at 500°C). The amount of Al intercalated into host mica crystals was measured by gravimetric analysis of Al_2O_3 and SiO_2 after the pillared mica powders were fused with Na_2CO_3 .

The APM powders (1.0 g) were treated with 100 mL of sulfuric acid. The concentration of sulfuric acid was varied from 0.1 to 2.5 mol/L. The acid-treatment was performed at 25°C for 0.5-36 h. After the acid-treatment, the products were washed several times with distilled water and then dried at 60°C.

Basal spacings of the APMs and the acid-treated products were measured by powder X-ray diffraction (XRD). The BET specific surface area, total pore volume and pore size distribution of the

products were evaluated from N₂ adsorption-desorption isotherms at liquid nitrogen temperature. The pore size distribution was determined by the BJH method [27] using the adsorption branch of the isotherms. The micropore size distribution was also determined by the Horvath-Kawazoe (HK) method [28] assuming slit-shaped pores for the typical products. Quantitative analysis of eluted Mg²⁺ and Al³⁺ ions was carried out by using inductively coupled plasma (ICP) spectrometry. The microstructure of the leached samples were also characterized by scanning electron microscopy (SEM) and transmission electron microscopy (TEM).

3. Results and discussion

3.1 Properties of alumina-pillared fluorine mica powders

Figure 1 shows XRD patterns of the pillared micas obtained at different calcination temperatures. APM-350 and APM-500 gave a sharp (001) profile. The (001) profile of APM-500 was broad and slightly shifted to higher diffraction angles compared with that of APM-350. In addition, APM-500 tended to lose high-order (00*l*) reflections. The basal spacings of APM-350 and APM-500 were 1.88 and 1.80 nm, respectively. PHA cations as a pillar precursor are known to convert into rigid oxide pillars in the interlayer regions of the host mica crystals at 300-500°C [29]. Thus, dehydration and dehydroxylation of the pillar precursor to form alumina pillars may be incomplete for APM-350 although the regularity of layer stacking sequences was high. The (001) reflection disappeared in the case of APM-700, indicating the

collapse of the pillared structure at calcination temperatures above 700°C.

Flaky crystals having a layer stacking structure were observed for APM-500 powders by SEM; the maximum dimensions parallel and perpendicular to the layers were about 30 μm and 2 μm , respectively, as described in our previous reports [4,6]. The Al content for APMs was estimated to be 2.27 mol (Al) per mol of Si_4O_{10} by gravimetric analysis.

Some properties of the APMs obtained under different calcination temperatures are listed in Table 1. APM-350 had a smaller specific surface area and pore volume than APM-500, while APM-350 had a slightly longer basal spacing than APM-500. This implies that dehydration and dehydroxylation of intercalated PHA cations were not completed for APM-350. APM-700 almost lost its porous nature owing to the collapse of the pillared phase. After a 1-hour acid-treatment using 1.0 mol/L H_2SO_4 , the specific surface area and total pore volume of APM-350 decreased, while those of APM-500 and APM-700 increased. The increase in the pore volume of APM-500 was particularly marked. These results suggested that APM-500 was an appropriate precursor for obtaining porous solids having a large specific surface area and total pore volume through acid treatment.

3.2 Mesopore formation and pore properties of the acid-treated products

Figure 2 shows the BET specific surface area and total pore volume of acid-treated products obtained from APM-500 under

different acid concentrations for 1 h. The specific surface area of the product decreased for an acid concentration of 0.1 and 0.5 mol/L, and then increased to >300 m²/g upon treating with 1.5 mol/L H₂SO₄. A slight decrease in surface area was observed for acid-treated products obtained by using >2.0 mol/L H₂SO₄. The total pore volume of the acid-treated products also decreased first and then increased as the acid concentration increased. These results indicate that pore properties of APM-500 powders are modified by the acid-treatment, depending on the acid concentration: the appropriate concentration for obtaining a large specific surface area is found to be 1.5 mol/L, where an acid-leaching time of 1 h is employed.

Pesquera et al. pointed out that the specific surface area of acid-treated montmorillonite reached maximum at a certain acid concentration and higher acid concentration prevented the evolution of porosity by passivation [18]. The acid-treatment of the APM-500 using higher concentration of acid than 2.5 mol/L may also be less effective for obtaining a large specific surface area product.

Figure 3 shows BET specific surface area and total pore volume plotted against acid-treatment time for the products obtained from APM-500. The acid concentration was fixed at 1.5 mol/L. For reference, Fig. 3 also plots the data for acid-treated products obtained from Na-TSM under the same conditions. Specific surface area of the acid-treated APM-500 sample decreased to 120 m²/g for an acid-treatment time of 0.5 h, and then increased to a

maximum of 410 m²/g for 2 h. Specific surface area decreased again for a 3-h treatment and then retained almost a constant value for treatment times longer than 3 h. Total pore volume also decreased for the product treated for a short time, and then increased to >0.3 cm³/g. These results indicate that the acid-treatment of APM powders alters their pore structure and leads to the formation of porous solids whose pore structure is very different from that of the pillared micas.

The acid-treatment of Na-TSM also led to an increase in specific surface area and pore volume although the values for acid-treated Na-TSM were much smaller those for acid-treated APMs. Several studies have been conducted on the acid leaching of swellable or non-swellable clay minerals to obtain porous solids [13-24]. These studies have yielded porous silica having micro- or mesopores depending on both the species of starting clay mineral and the leaching conditions. For example, montmorillonite led to the formation of porous silica having mesopores with a specific surface area of ca. 200 m²/g [19], and phlogopite, a naturally occurring mica, led to the formation of porous silica having micro- and mesopores with a maximum specific surface area of >500 m²/g, depending on the leaching conditions [16]. However, the reported leaching conditions were mostly intense, employing higher acid concentrations and/or raised temperatures. By contrast, the acid-leaching conditions in the present study were milder. Although saponite, a magnesian silicate like Na-TSM, led to the formation of high surface area solids exceptionally under mild

acid-treatment conditions [23,24], Na-TSM having much larger particle size didn't alter into high surface area solids under the mild acid-leaching. These facts indicate that the acid-treatment of APM-500 has an advantage over that of the non-pillared clay minerals including Na-TSM because modification of pore properties can be achieved under milder conditions.

Figure 4(a) shows typical N₂ adsorption-desorption isotherms for the products. The isotherm of the APM-500 sample before the acid-treatment was of type I according to the IUPAC classification [30]. The product obtained by the 0.5-h acid-treatment also gave a type I isotherm, but the adsorption volume was lowered. In contrast, the products acid-leached for 2 h gave mixed isotherms, corresponding to a combination of types I and IV, which is indicative of the formation of mesopores. The hysteresis loop of the isotherm was similar to type H4 [30], corresponding to slit-shaped pores.

Figure 4(b) shows the pore size distribution curves (BJH method [27]) of the products obtained from APM-500 using 1.5 mol/L H₂SO₄ for different leaching times. The curve for APM-500 before the acid-treatment gave a shoulder in the small diameter region below 2 nm, which constitutes part of the micropore distribution curve. The shoulder almost disappeared after acid leaching for 0.5 h, indicating that the micropores have largely vanished. The decrease in specific surface area and total pore volume during the initial stage of acid leaching was attributable to the decline in microporosity in APM-500. This can be

ascertained by the change in micropore distribution curves obtained by the HK method [28] using a slit-like pore model, which are shown in Fig. 5; the APM-500 micropores almost vanished as a result of acid-leaching for 0.5 h.

An indication of mesopore formation below 5 nm appeared in the case of the product obtained after acid leaching for 1 h (Fig. 4(b)). A marked formation of mesopores, which gave a peak at a pore diameter of around 3.2 nm, was observed after acid leaching for 2 h. The peak broadened and shifted to larger pore diameters as the acid-leaching time was prolonged. Furthermore, the micropores, which have slightly smaller pore sizes than those of the mother APM-500, were re-formed by the acid leaching in the case of leaching times longer than 2 h (Fig. 5). The smaller-sized micropores also contribute to the increase in specific surface area.

Figure 6 shows XRD patterns of acid-treated products obtained from APM-500 at different leaching times. APM-500 gave rational (00 l) reflections, indicating the formation of a pillared structure with a basal spacing of 1.80 nm. However, even in the case of the short treatment time of 0.5 h, the product lost its sharp diffraction peaks, exhibiting a smaller basal spacing of ca. 1.4 nm. Acid-treated products obtained by leaching for longer than 1 h gave no basal reflections, although they showed small-angle scattering below $2\theta = 3^\circ$. These results show that the acid-treated products almost lose their interlayer pillared structure and the regularity of their layer stacking sequence in the early stages of the acid-leaching process.

The fraction of Al^{3+} and Mg^{2+} cations that leached out of APM-500 during the acid-treatment is plotted against the leaching time in Figure 7. The early stages of the acid-treatment favored the elution of Al^{3+} ions. The steep increase in the elution of Al^{3+} came to an abrupt end at 2 h. The amount of leached Mg^{2+} ions, which was estimated on the basis of the original Mg^{2+} content in APM-500, increased to 54% after acid-leaching for 2 h and then reached a constant value of ~75% for >12 h. The SiO_2 content of products after acid leaching for 2 and 36 h was 69 and 76 mass%, respectively. Thus, the SiO_2 content of the present products was quite low compared with those reported in studies on the acid leaching of clay minerals (typically >90 mass% SiO_2) [13,14,16,17,21,22].

Na-TSM used as host mica crystal has no Al^{3+} substitution in the silicate layer so that the elution of Al^{3+} ions was attributable entirely to those leached out from alumina pillars in the interlayer regions. In the early stage of acid leaching, the products almost lost their regular interlayer pillared structure and microporous nature owing to the partial dissolution of the alumina pillars. As the acid-leaching time was prolonged, the formation of mesopores occurred with the abrupt leaching of octahedral Mg^{2+} ions. Thus, the leaching of Mg^{2+} ions from octahedral sheets of the silicate layer seems to be key in the formation of mesopores.

Okada et al. pointed out that AlO_4 substitution in the SiO_4 tetrahedral sheets of the silicate layer has considerable influence

on the leaching rate of the various minerals [22]. Since SiO_2 has a greater resistance to acid, the rate of acid leaching of talc, which has no Al substitution in the SiO_4 tetrahedral sheets and is a non-swelling clay mineral, is very slow and the leached products from talc are nonporous [21]. Kaviratna and Pinnavaia, however, reported the formation of high-surface-area ($>150 \text{ m}^2/\text{g}$) products by acid-treatment at 60°C from swelling fluorohectorite, which has no Al substitution in its tetrahedral sheets, either [15]. Microporous APMs have interlayer regions propped by alumina pillars so that water molecules and protons are able to diffuse into the interlayer regions of APMs. Thus, it is presumably the interlayer water and protons that allow acid leaching of APMs under milder conditions.

Judging from the hysteresis type of isotherm, the mesopores in the present acid-leached products seem to have a slit-like shape. Upon leaching of Mg^{2+} ions, the planar silicate layers of the mica presumably become corrugated at the nanoscale, resulting in the formation of slit-like mesopores between the corrugated layers along with smaller micropores.

The cation exchangeability for the product obtained by a 2-h acid-treatment using $1.5 \text{ mol/L H}_2\text{SO}_4$ was examined using $0.05 \text{ mol/L NiSO}_4$ solution by the same procedure as the previous report [4]; $0.21 \text{ mmol}/(\text{g acid-treated product})$ of Ni^{2+} ions were incorporated into the product.

3.3 SEM and TEM observations of the products

Figures 8(a)-(c) show SEM images of the products before and

after the acid-treatment. The initial flaky morphology and dimensions of the products were almost fully retained, even after prolonged (36 h) acid leaching. The edges of mica flakes along cleavage lines became somewhat rough as the acid-leaching time was prolonged. Moreover, small deposits were observed on the flakes in the case of the product obtained by the 36-h acid-leach. This suggests that the acid attacked the edges as well as the internal surface during the acid-treatment of APM. The XRD results indicated the collapse of the interlayer pillared structure upon acid-treatment. However, on the basis of their morphologies, the nano-corrugated mica layers, which were formed as a result of the Mg^{2+} leaching, may topotactically have loose stacking sequences inherited from the mother APMs, accompanying the mesopore formation. Figure 8(d) shows a TEM image of the product obtained by the 2-h acid-treatment. Lighter contrast regions, several nanometers in size, were observed in the flake. The size of these regions agrees well with the mesopore size evaluated by the BJH method. The electron diffraction of the acid-leached product showed an amorphous halo pattern (Fig. 8d), while that of APM-500 showed a spot pattern (not shown). These SEM and TEM observations indicate that the elution of cation constituents under mild acid-treatment conditions retained the flaky morphology and the slit-shaped mesopores were formed on the inside of the flakes.

Thus, mild acid-treatment using APMs is a useful route for obtaining unique mesoporous solids retaining the large particle

sizes of the mother synthetic micas.

4. Conclusions

Alumina-pillared fluorine micas were acid-treated at 25°C under different conditions. The acid-treatment led to the collapse of the interlayer pillared structure with a basal spacing of 1.8 nm and the formation of mesoporous solids. The product obtained by a 2-h acid-treatment using 1.5 mol/L H₂SO₄ gave a specific surface area of 410 m²/g, a total pore volume of >0.31 cm³/g and a unimodal pore size distribution around 3.2 nm. Prolongation of the acid-treatment time led to an increase in the mesopore size. Upon acid-treatment, Al³⁺ and Mg²⁺ cations were eluted from the pillared mica. The elution of octahedral Mg²⁺, in particular, is key to the formation of mesopores. The flaky morphology of the acid-leached products was inherited from the mother pillared mica. This indicates that the elution of constituent cations and the concomitant formation of mesopores occurs through a topotactic process under mild acid-treatment conditions. This represents a novel process for obtaining unique porous solids.

References

- 1) K. Ohtsuka, Y. Hayashi, M. Suda, Chem. Mater. 5 (1993) 1823.
- 2) T. Yamaguchi, Y. Sakai, K. Kitajima, J. Mater. Sci. 34 (1999) 5771.
- 3) T. Yamaguchi, A. Shirai, S. Taruta, K. Kitajima, Ceram.-Silik. 45 (2001) 43.

- 4) T. Yamaguchi, K. Kitajima, E. Sakai, M. Daimon, *Clay Miner.* 38 (2003) 41.
- 5) T. Yamaguchi, K. Kitajima, E. Sakai, M. Daimon, *J. Ceram. Soc. Japan* 111 (2003) 567.
- 6) T. Yamaguchi, T. Ito, Y. Yajima, S. Taruta, K. Kitajima, *J. Ceram. Soc. Japan* 112 (2004) S21.
- 7) K.-i. Shimizu, Y. Nakamuro, R. Yamanaka, T. Hatamachi, T. Kodama, *Microporous Mesoporous Mater.* 95 (2006) 135.
- 8) T. Yamaguchi, S. Taruta, T. Yamakami, K. Kitajima, *Mater. Res. Bull.* in press. (doi: 10.1016/j.materresbull.2007.01.009)
- 9) K. Kitajima, N. Daimon, *Nippon Kagaku Kaishi* (1975) 991.
- 10) K. Kitajima, F. Koyama, N. Takusagawa, *Bull. Chem. Soc. Jpn.* 58 (1985) 1325.
- 11) T. Kodama, Y. Harada, M. Ueda, K.-i. Shimizu, K. Shuto, S. Komarneni, W. Hoffbauer, H. Schneider, *J. Mater. Chem.* 11 (2001) 1222.
- 12) K.-i. Shimizu, K. Hasegawa, Y. Nakamuro, T. Kodama, S. Komarneni, *J. Mater. Chem.* 14 (2004) 1031.
- 13) K. Okada, A. Shimai, T. Takei, S. Hayashi, A. Yasumori, K.J.D. MacKenzie, *Microporous Mesoporous Mater.* 21 (1998) 289.
- 14) J. Temuujin, G. Burmaa, J. Amgalan, K. Okada, Ts. Jadambaa, K.J.D. MacKenzie, *J. Porous Mater.* 8 (2001) 233.
- 15) H. Kaviratna, T.J. Pinnavaia, *Clays Clay Miner.* 42 (1994) 717.
- 16) K. Okada, N. Nakazawa, Y. Kameshima, A. Yasumori, J. Temuujin, K.J.D. MacKenzie, M.E. Smith, *Clays Clay Miner.*

- 50 (2002) 624.
- 17) J. Temuujin, K. Okada, K.J.D. MacKenzie, *Appl. Clay Sci.* 22 (2003) 187.
 - 18) C. Pesquera, F. González, I. Benito, C. Blanco, S. Mendioroz, J. Pajares, *J. Mater. Chem.* 2 (1992) 907.
 - 19) T. Shinoda, M. Onaka, Y. Izumi, *Chem. Lett.* (1995) 495.
 - 20) J. Temuujin, K. Okada, Ts. Jadambaa, K.J.D. MacKenzie, J. Amarsanaa, *J. Mater. Sci. Lett.* 21 (2002) 1607.
 - 21) K. Okada, J. Temuujin, Y. Kameshima, K.J.D. MacKenzie, *Clay Sci.* 12 (2003) 159.
 - 22) K. Okada, N. Arimitsu, Y. Kameshima, A. Nakajima, K.J.D. MacKenzie, *Appl. Clay Sci.* 30 (2005) 116.
 - 23) O. Prieto, M.A. Vicente, M.A. Bañares-Muñoz, *J. Porous Mater.* 6 (1999) 335.
 - 24) M. Suárez Barrios, C. de Santiago Buey, E. García Romero, J.M. Martín Pozas, *Clay Miner.* 36 (2001) 483.
 - 25) R. Ishii, M. Nakatsuji, K. Ooi, *Microporous Mesoporous Mater.* 79 (2005) 111.
 - 26) T. Fujita, K. Kitajima, S. Taruta, N. Takusagawa, *Nippon Kagaku Kaishi* (1993) 319.
 - 27) E.P. Barrett, L.G. Joyner, P.P. Halenda, *J. Am. Chem. Soc.* 73 (1951) 373.
 - 28) G. Horvath, K. Kawazoe, *J. Chem. Eng. Japan.* 16 (1983) 470.
 - 29) P. Cool, E.F. Vansant, in: H.G. Karge, J. Weitkamp (Eds), *Molecular Sieves*, vol. 1, Springer, 1998, pp.265-288. (ISBN 3-540-63622-6).

- 30) K.S.W. Sing, D.H. Everett, R.A.W. Haul, L. Moscou, R.A. Pierotti, J. Rouquerol, T. Siemieniowska, *Pure Appl. Chem.* 57 (1985) 603.

Figure captions

Fig. 1 XRD patterns of alumina-pillared fluorine micas (APMs) used for acid-treatment. (a) APM-350, (b) APM-500 and (c) APM-700.

Fig. 2 The BET specific surface area and total pore volume of the products versus acid concentration. (Acid-leaching time: 1 h)

Fig. 3 The BET specific surface area and total pore volume of the products versus acid-leaching time. (Acid concentration: 1.5 mol/L)

Open circles indicate the values for the products obtained from Na-TSM by acid-treatment.

Fig. 4 (a) Typical isotherms and (b) pore size distribution curves (BJH method) of products obtained from APM-500 by acid-treatment using 1.5 mol/L H_2SO_4 for different times.

Fig. 5 Micropore size distribution curves (HK method) of the products obtained from APM-500 by acid-treatment using 1.5 mol/L H_2SO_4 for different times.

Fig. 6 XRD patterns of products using 1.5 mol/L H_2SO_4 for different times.

Fig. 7 Fraction of eluted Al^{3+} and Mg^{2+} versus acid-leaching times. (Acid concentration: 1.5 mol/L)

Fig. 8 SEM and TEM micrographs of the products. (a) SEM image of the starting pillared mica (APM-500); (b) and (c) SEM images of the acid-treated products obtained using 1.5 mol/L H_2SO_4 solution for 2 and 36 h, respectively, and (d) TEM image of the product obtained by a 2-h acid-treatment using 1.5 mol/L H_2SO_4 .

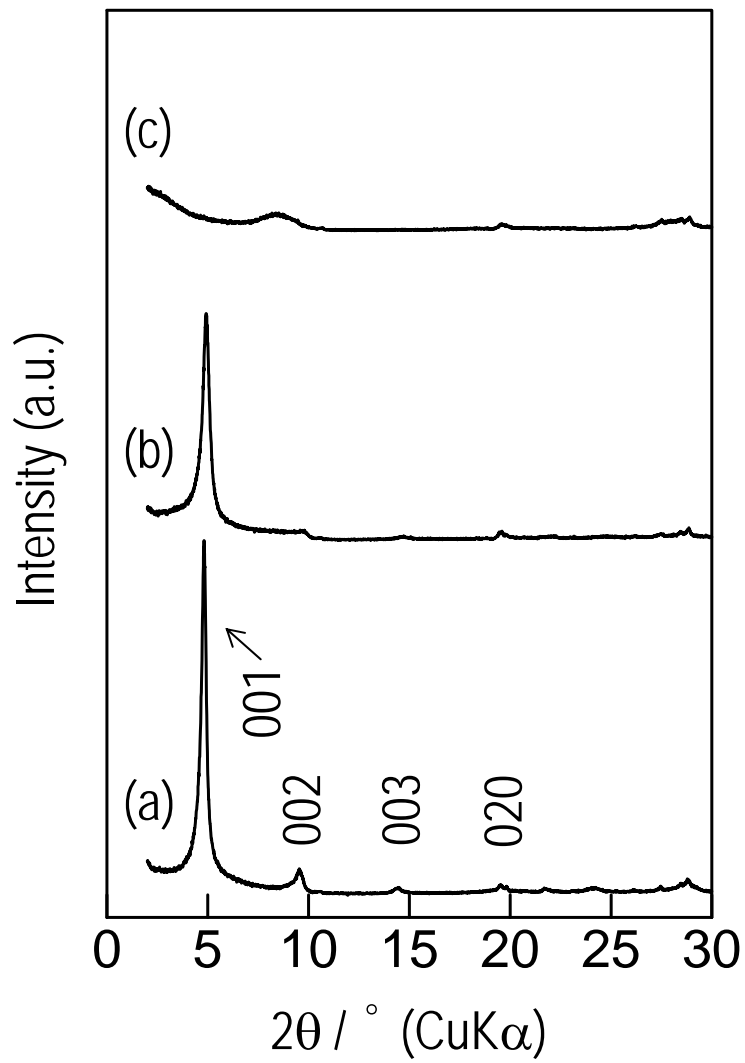


Fig. 1

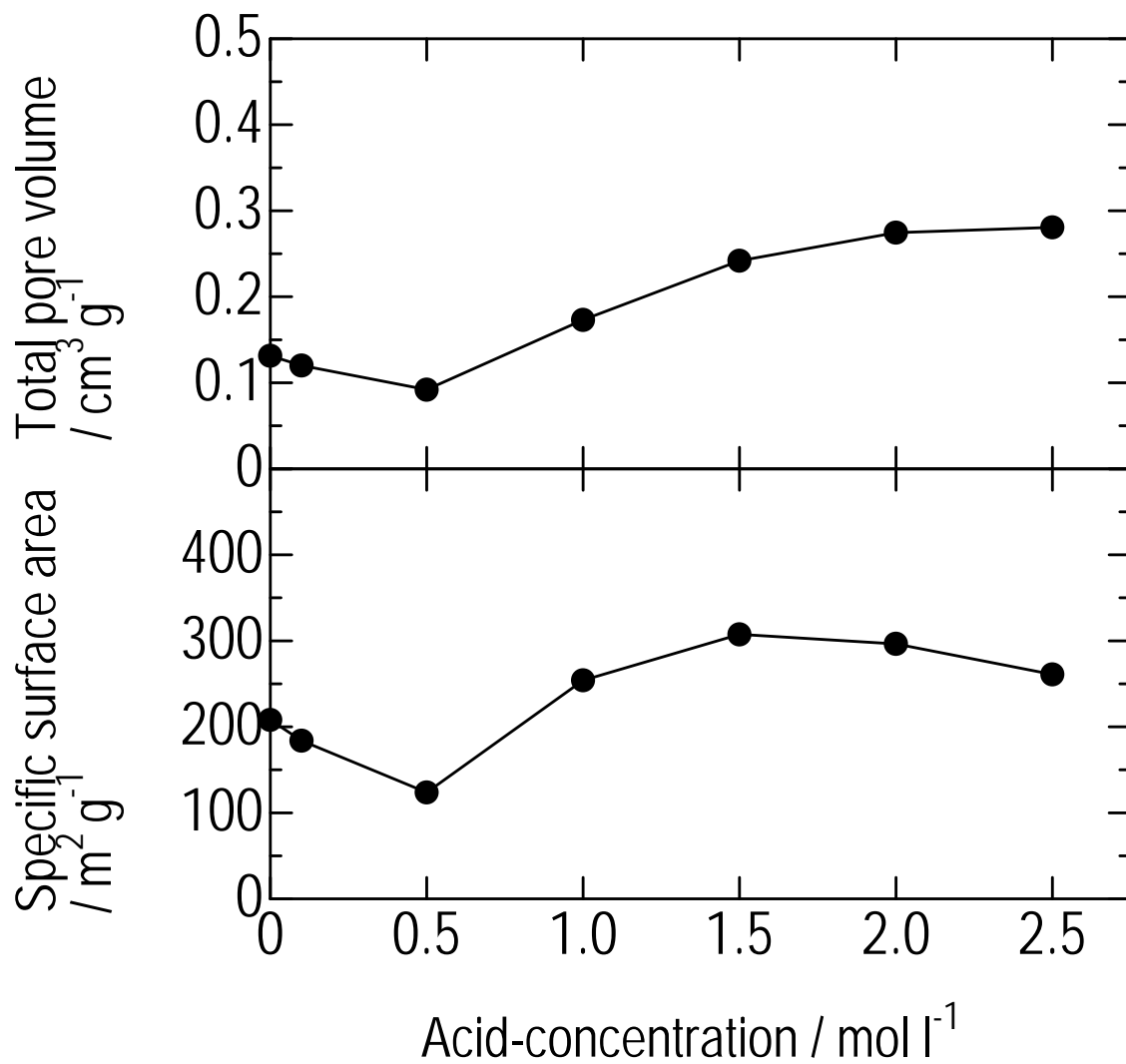


Fig. 2

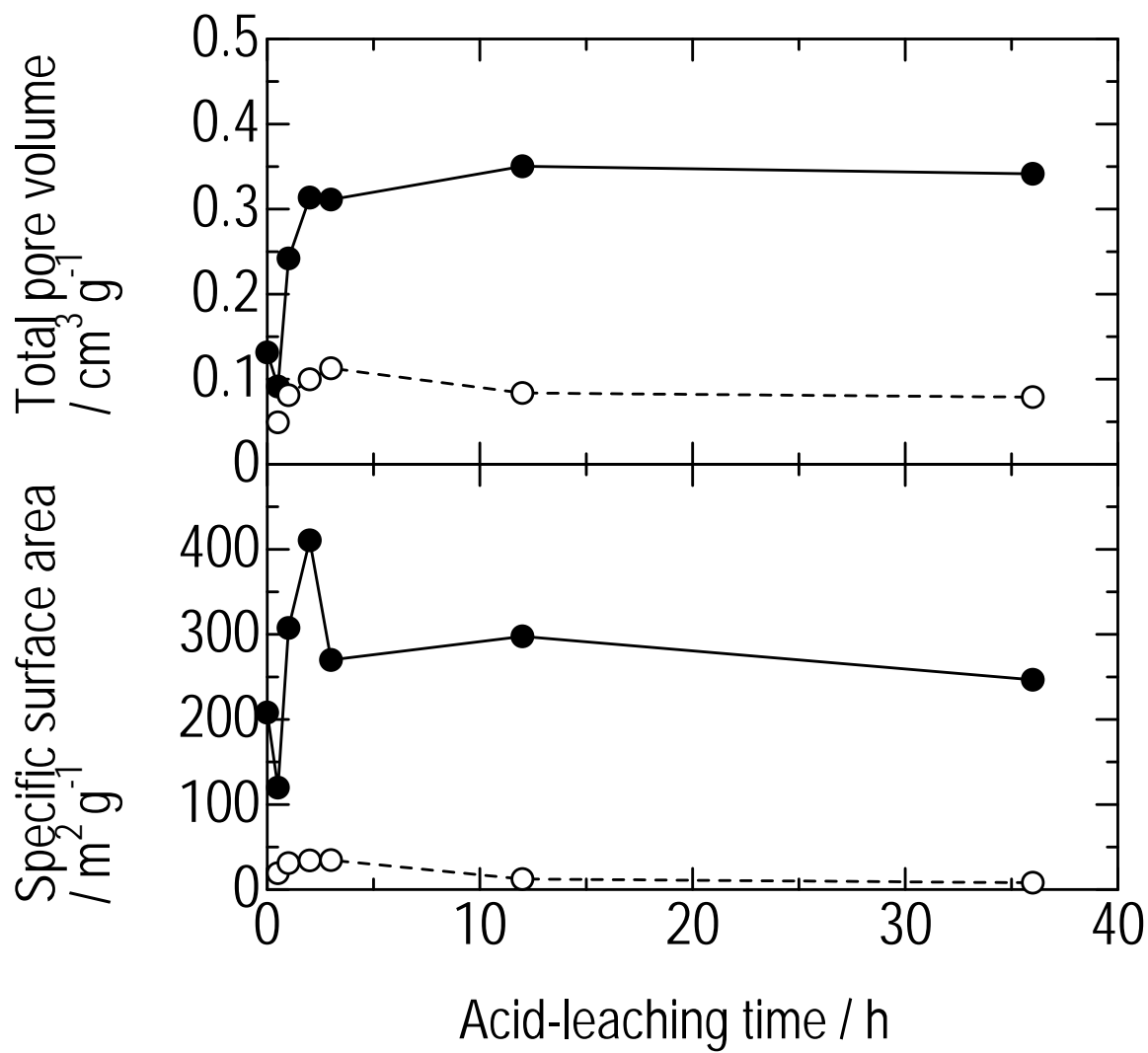


Fig. 3

(a)

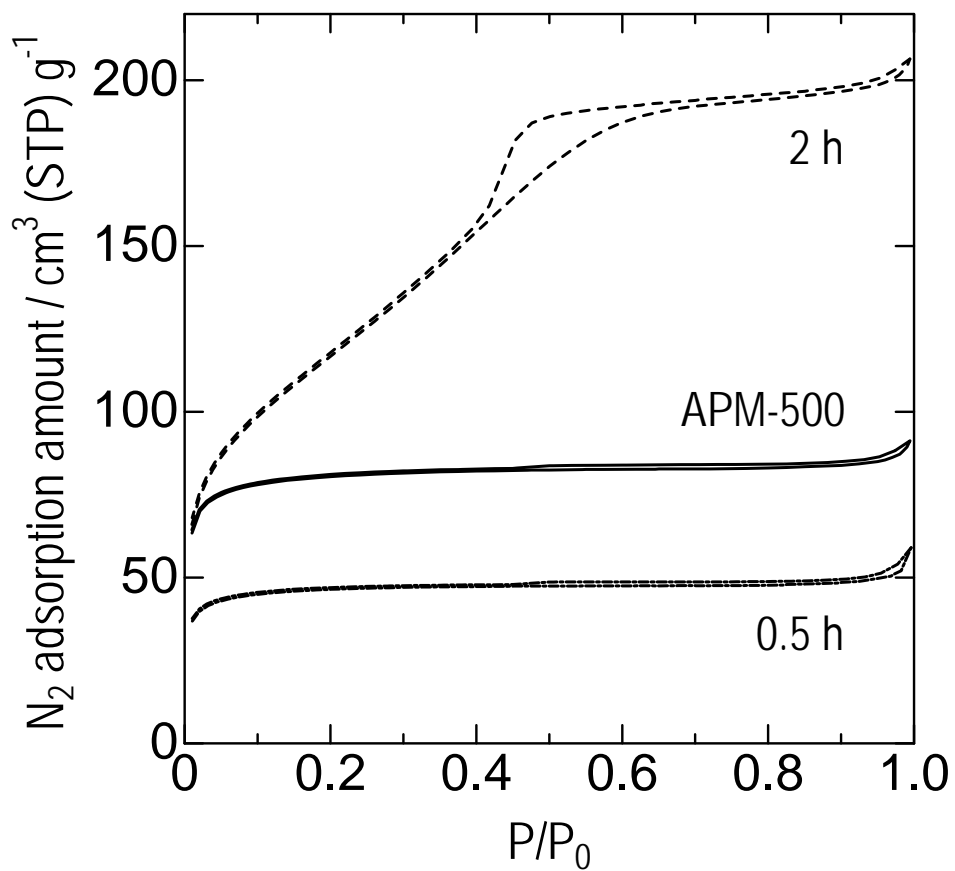


Fig. 4(a)

(b)

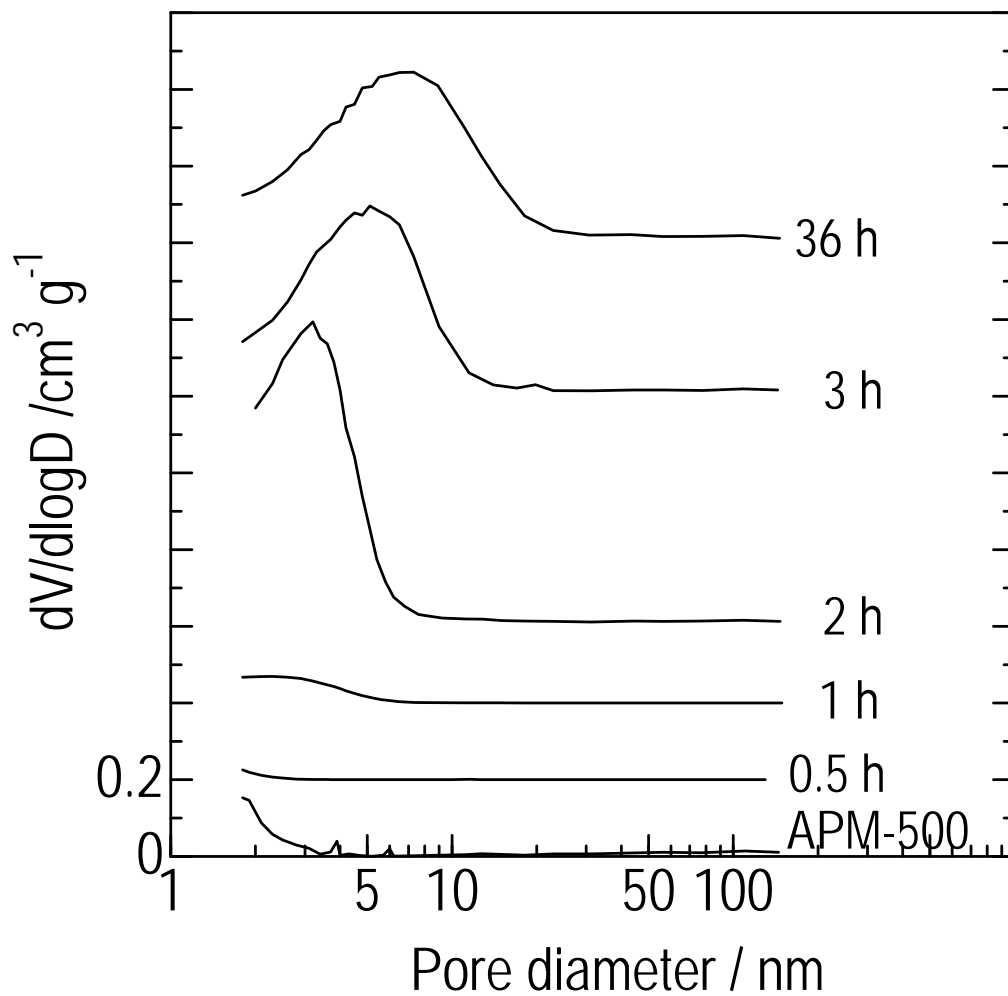


Fig. 4(b)

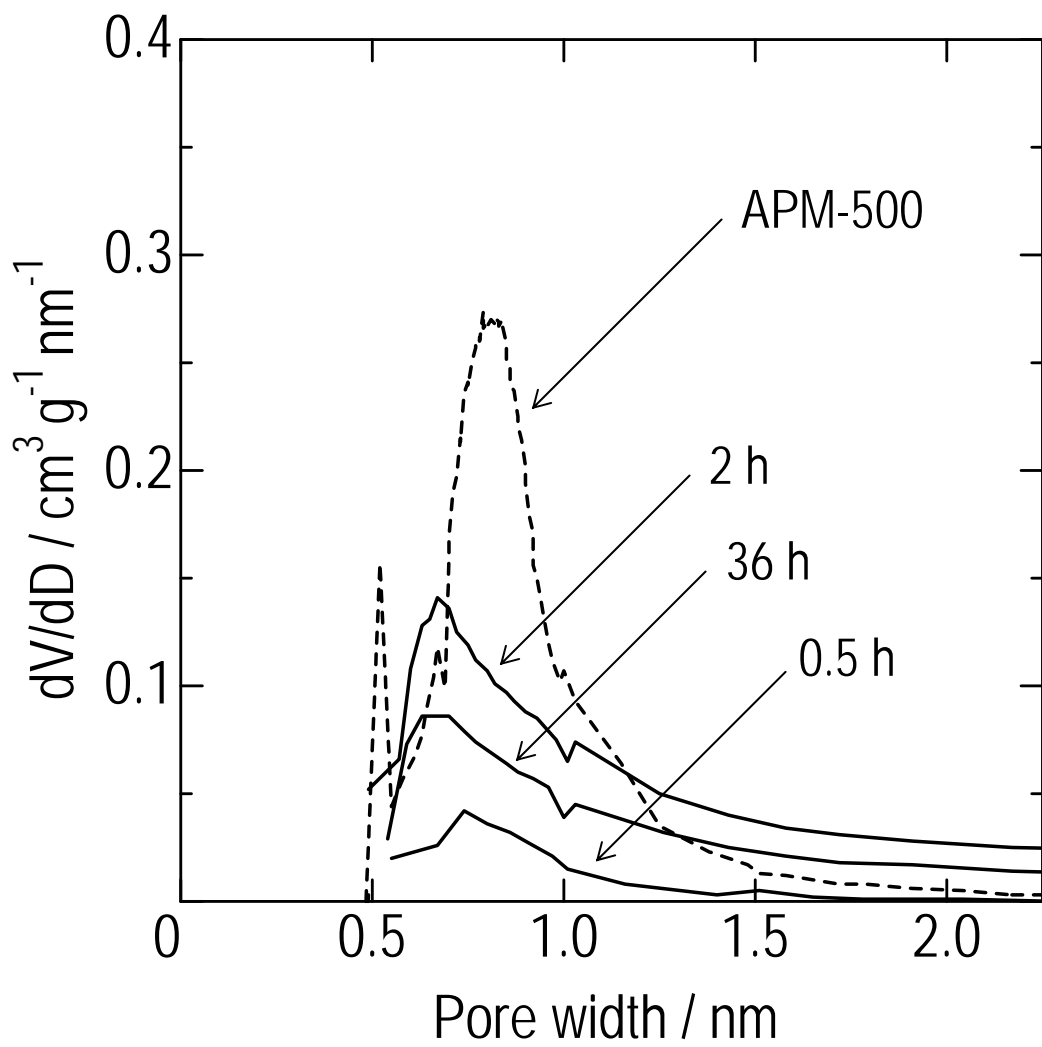


Fig. 5

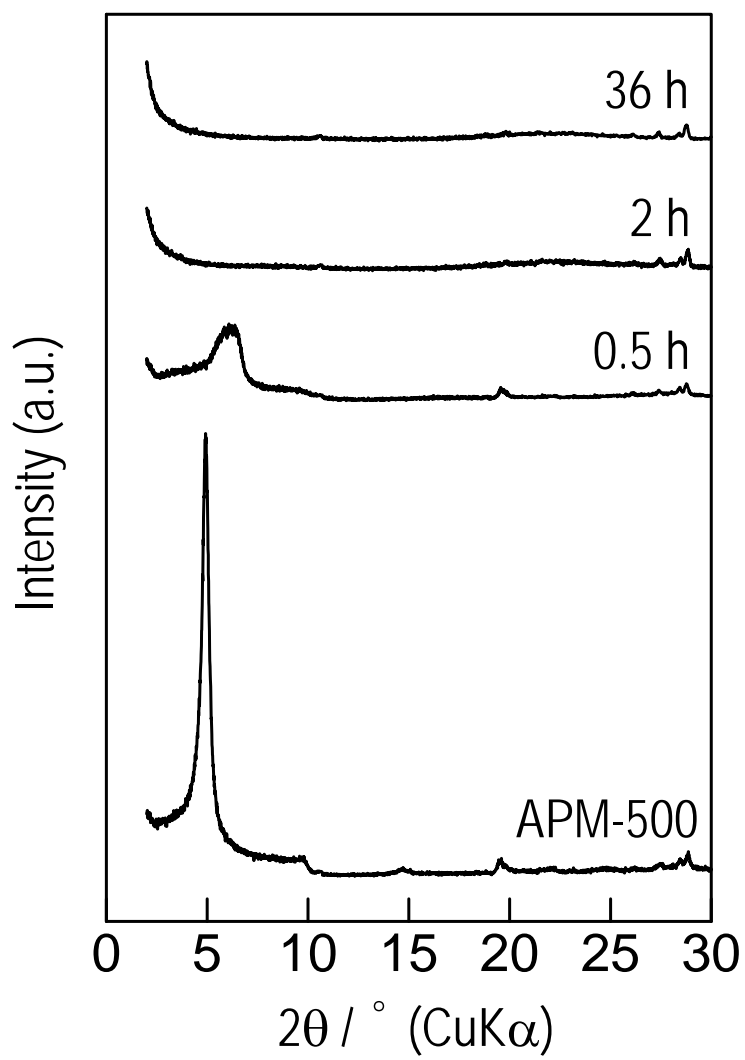


Fig. 6

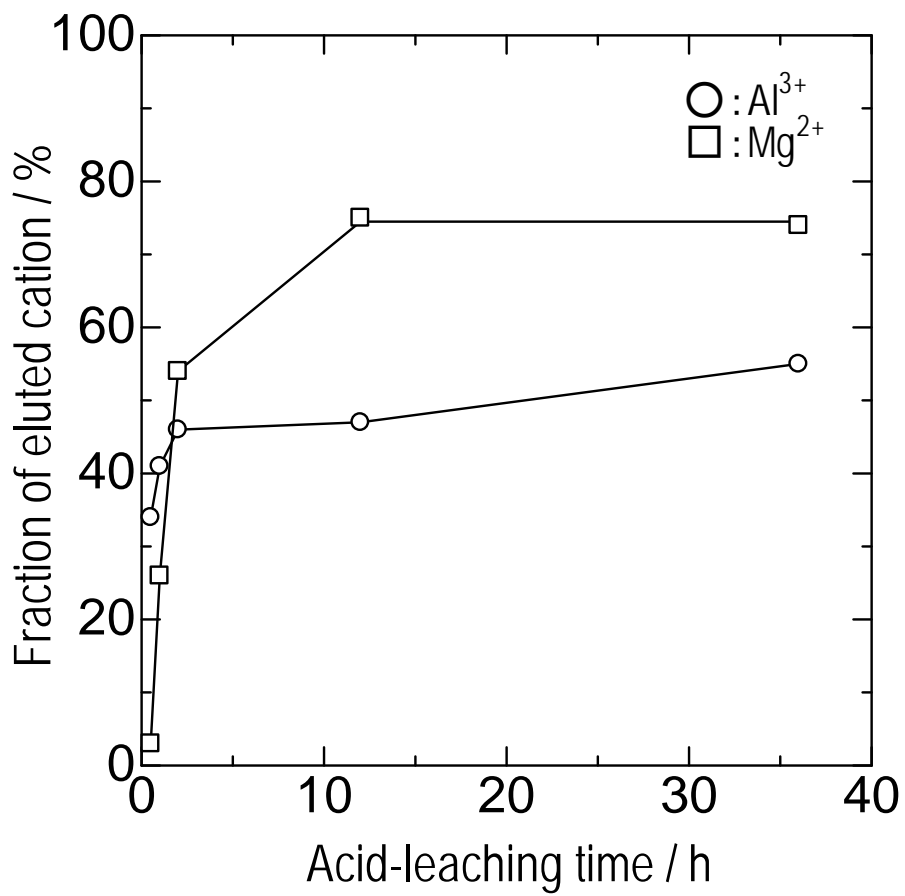


Fig. 7

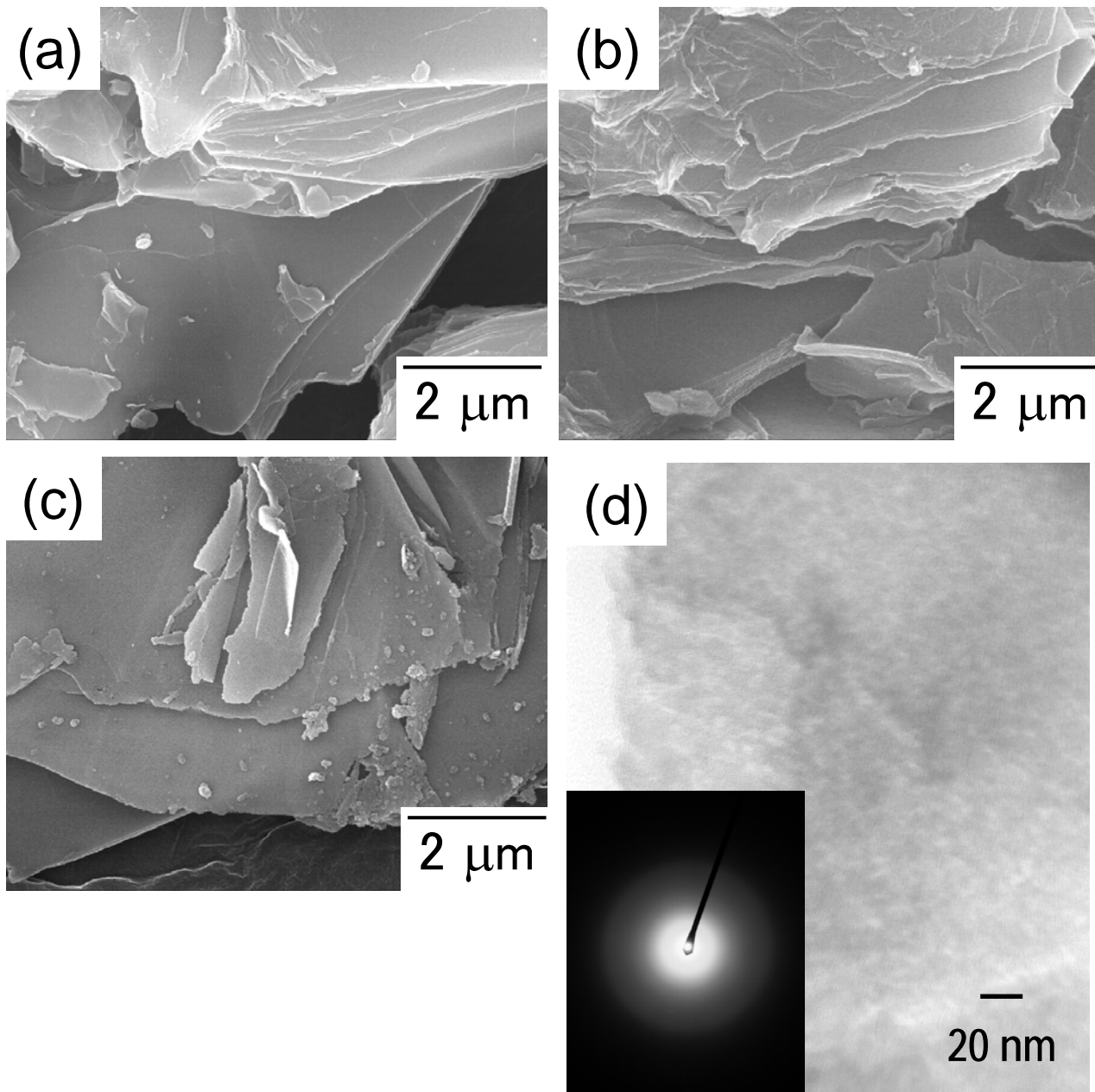


Fig. 8

Table 1 Properties of alumina-pillared micas

Sample	Calcination temperature (°C)	Basal spacing (nm)	Before acid-treatment		After acid-treatment*	
			BET specific surface area (m ² /g)	Total pore volume (cm ³ /g)	BET specific surface area (m ² /g)	Total pore volume (cm ³ /g)
APM-350	350	1.88	183	0.12	112	0.07
APM-500	500	1.80	208	0.13	254	0.17
APM-700	700	-	5	0.01	82	0.06

*: Acid-treatment condition: 1.0 mol/L H₂SO₄, for 1 h.